Entropy parameters for falling film absorber optimization

ENTROPY PARAMETERS FOR FALLING FILM ABSORBER OPTIMIZATION

Niccolò Giannetti[a*], Andrea Rocchetti[b], Arnas[a], Kiyoshi Saito[a], Seiichi Yamaguchi[a]

[a] Department of Applied Mechanics and Aerospace Engineering, Waseda University, 3-4-1 Okubo, Shinjuku-ku, Tokyo 169-8555, Japan

[b] DIEF - Department of Industrial Engineering of Florence, Via Santa Marta, 3; 50139 Firenze, Italy

[*]Corresponding Author: Niccolo` Giannetti; e-mail address: niccolo@aoni.waseda.jp

Keywords: Entropy generation; Irreversibility; Falling film; Absorber; Horizontal tube; Optimization.

Abstract

A local entropy generation analysis, for water vapor absorption in LiBr-H_2O solution, is performed referring to velocity, temperature and concentration fields obtained from the numerical solution of mass and energy transport equations. The hydrodynamic description is based on Nusselt boundary layer and the actual amount of irreversibility introduced is determined for a falling film over a cooled horizontal tube inside the absorber. Results are explored in different operative conditions, in order to examine the impact of the various irreversibility sources in a wide operative range. A least irreversible solution mass flow-rate can always be identified. Furthermore, a simple and general thermodynamic analysis, carried out regarding a refrigerating and a heat boosting applications of absorption systems, makes evidence of a dimensionless group "$Q/\sigma T$" that separates the weight of the irreversibilities and gives the way to an optimization criterion applied to the absorber in order to improve the whole system efficiency. Both equilibrium condition and sub-cooling of the solution at the inlet are considered for typical temperature and concentration of refrigerators' absorbers and heat transformers' absorbers. Results suggest the importance to work at reduced mass flow-rates

with a thin uniform film both for refrigerators and heat transformers. In practice, tension-active additives are required to realize this condition. Also, it is highlighted that, for a fixed operative Reynolds, the two parameters defined with reference to the dimensionless group "$Q/\sigma T$" can be maximized by specific values of the tube radius, solution sub-cooling and temperature difference between the wall and the inlet solution.

Nomenclature

a	Thermal diffusivity [m^2s^{-1}]
C	Molar concentration [$mol \cdot m^{-3}$]
c_p	Isobaric molar heat [$J \cdot mol^{-1}K^{-1}$]
D	Mass diffusivity [m^2s^{-1}]
DA	Dimensionless absorption flux at the interface
DQ	Dimensionless heat flux at the wall
E	Entropy generation rate per tube unit length [$W \cdot m^{-1}K^{-1}$]
g	Gravity [$m \cdot s^{-2}$]
G	Mass flux per unit surface [$kg \cdot m^{-2}s^{-1}$]
h	Molar enthalpy [$J \cdot mol^{-1}$]
H	Number of nodes in radial direction
i	Specific enthalpy [$J \cdot kg^{-1}$]
j	Molar flux [$mol \cdot m^{-2}s^{-1}$]
k	Thermal conductivity [$W \cdot m^{-1}K^{-1}$]
L	Mechanical power [W]
m	Mass Flow-rate [$kg \cdot s^{-1}$]
M	Molar weight [$kg \cdot mol^{-1}$]

N	Number of nodes in tangential direction
P	Pressure [kPa]
Q	Thermal power [W]
q	Heat flux per tube unit length [$kW \cdot m^{-1}$]
r	Outer tube radius [m]
R	Grid ratio in normal direction
Re	Reynolds Number
S	Volumetric entropy generation rate [$W \cdot m^{-3}K^{-1}$]
s	Molar entropy [$J \cdot mol^{-1}K^{-1}$]
T	Temperature [K]
u	Stream-wise velocity [$m \cdot s^{-1}$]
v	Radial velocity [$m \cdot s^{-1}$]
V	Total velocity [$m \cdot s^{-1}$]
x	Local tangential position [m]
y	Local normal position [m]
Z	Tube length [m]

Greek symbols

Γ	Mass flow rate per unit length [$kg \cdot s^{-1}m^{-1}$]
Λ	Absorbed vapor per unit length of the tube [$kg \cdot s^{-1}m^{-1}$]
β	Stream-wise Angle [rad]
δ	Film Thickness [m]
ε	Dimensionless tangential position
ϕ	General parameter identification
γ	Chemical potential [$J \cdot mol^{-1}$]

η	Dimensionless normal position
η_{Ca}	Carnot efficiency
μ	Viscosity [Pa·s]
θ	Dimensionless temperature
ρ	Density [kg·m^{-3}]
σ	Irreversibility rate [W·K^{-1}]
τ	Shear stress tensor [Pa]
ω	LiBr mass concentration

Subscripts

0	Standard condition
A	Absorber
abs	Absorption
C	Condenser
c	Convection
CH	Chiller
d	Diffusion
E	Evaporator
e	Equilibrium
f	Friction
g	Global
G	Generator
H2O	Water
HT	Heat transformer
HP	Heat pump

i,j	Node indexes
if	Interface
in	Inlet
min	Minimum
RM	Refrigerating machine
TM	Thermal machine
out	Outlet
s	Sub-cooling
S	Solution
sat	Phases equilibrium
t	Thermal
v	Vapor
w	Wall

1. Introduction

Nowadays the awareness of the environmental issues of the planet steers towards clean and efficient energy conversion systems. Absorption chillers, heat pumps and heat transformers represent an opportunity in this direction. The use of the vapor absorption cycle for heat driven energy systems was among the first popular and widely used methods of refrigeration. Even though the development of vapor compression cycles has limited the implementation field of vapor absorption systems, the main benefits of absorption cycle are still evident: since a negligible amount of electricity is needed, waste heat can be used as the main energy source and higher reliability can be ascribed to the absence of moving parts. In addition, typically used refrigerant (water or ammonia) are not responsible of ozone depletion effect.

All the real processes occurring in an energy conversion system are associated to an unavoidable degradation of the original amount of energy. The second law of thermodynamics provides a qualitative description, which is not confined to engineering, and is critical to identify the limitations imposed to a physical process. Namely, according to this general design issue, thermal design and basic thermodynamics are to be employed together with the purpose of identifying the optimum size or operating regime of a certain engineering system, where by “optimum” the least exergy destroying condition, which can still assure the fundamental engineering function, is intended. Among the possible scenarios, the method of entropy generation minimization can be used to evaluate the irreversibility introduced, characterize the quality of energy-conversion, and develop consistent criteria for the optimization and control of the system. From this point of view, the enhancement of efficiency describing the achieved technological development constitutes a secondary result of entropy generation minimization [1] and entropy can be used to develop useful criteria for system optimization and control.

From the prospective of the global system, authors in [2] and [3] have presented a literature review of finite-time thermodynamics optimization of absorption refrigeration systems and analyzed the various possible objective functions. In general, in order to consider the temperature level of the various heat fluxes involved in the energy conversion process, a second law approach is particularly significant for the characterization of the performance of heat-driven systems. Exergy-based analyses of water-lithium bromide absorption refrigeration systems, in both their single [4] and multiple effect configurations [5], and absorption heat transformers [6], have been performed to evaluate performance and exergy loss of the system and its components.

The fundamental heat and mass-transfer processes constituting the absorption cycle are realized inside specific heat exchangers, whose characteristics have decisive effects on the overall system efficiency, on its dimensions and on its cost. In the conventional case of falling film heat exchangers,

high transfer coefficient and low pressure drop can be obtained. However, the attempt to experimentally and theoretically describe the complex heat and mass-transfer mechanism occurring inside these devices is still incomplete and has not leaded to conclusive approaches. As a rule, [4], [5], [6] and [7] have highlighted that the maximum exergy destruction occurs in the absorber and the analysis and optimization of this device is crucial for the absorption system in refrigerator and heat transformer applications.

In terms of modelling efforts, [8], [9], [10], [11] and [12] have discussed simplified models for falling film absorption of water vapor over a horizontal tube. Similarly, they solved the problem with a finite difference method and studied the effect of different parameters on the coupled heat and mass transfer processes.

To the authors' knowledge, few studies [1], [13], [14], [15] performing a second law analysis of absorption devices have been previously carried out. In particular, [16] and [17] report a second law-based analytical study for gas absorption into a laminar, gravity-driven, viscous, incompressible, isothermal liquid film. The main conclusion states that entropy generation is mainly ruled by the coupling effects between heat and mass transfer in proximity of the gas-liquid interface and by viscous irreversibility near the solid wall. However, heat transfer and the tube wall geometry have not been included in the problem. Simultaneous cooling and absorption allow the process to be maintained far from the thermodynamic equilibrium at which absorption won't occur any longer.

The main purposes of this work stem from the proper expression of the local entropy generation rate representing real LiBr-H_2O absorptive films. A local analysis can be carried out by means of the numerical solution of energy and species transport equations around a cooled horizontal tube. Since entropy generation minimization has been widely accepted as a method for heat exchangers' design and optimization, a parametric study based on entropy generation analysis is performed. Finally, a simple thermodynamic analysis shows that the absorption system performance can be improved by

means of the optimization of the absorber design and operational regime when suitable dimensionless groups, accounting for the total entropy generation introduced, are defined as objective parameters.

2. Model description and numerical solution

A single horizontal tube is considered and the LiBr-H_2O solution flows viscously down over it driven by gravity as a laminar incompressible liquid, while vapor mass transfer process occurs at the film interface. The heat released by the absorption is rejected to the cooling water flowing inside the tube. The system under analysis is schematically showed in Figure 1. Heat and mass transfer characteristics of the absorber tube have been obtained by numerically solving transport of mass and energy equations, under the following main assumptions:

- Steady and laminar flow without interfacial waves.
- Thermodynamic equilibrium with the vapor at the film interface.
- Negligible shear force between the liquid film and the vapor.
- Disturbance at the edges of the system are neglected assuming that both the tube circumference and length are large if compared to the film thickness.
- Physical properties are calculated with reference to the inlet values of concentration and temperature, but remain constant while the film is flowing on the tube.
- Negligible heat transfer to the vapor phase.
- Constant temperature of tube surface.
- Body fitted coordinates (x along the tube surface and y normal to it at any point) are used because the film thickness is small if compared to the tube circumference [12].

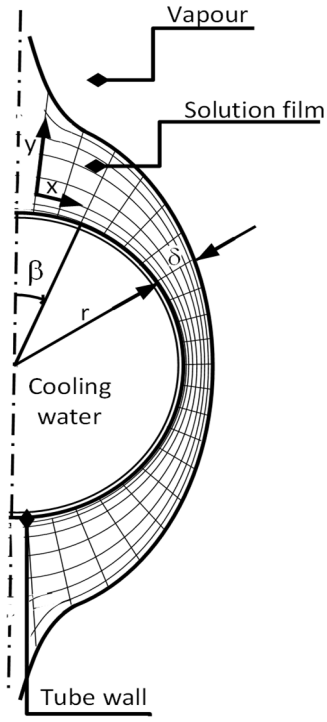

Figure 1 Local coordinate system of the flowing film

The tangential and normal velocity components (respectively, eqs. 1 and 2), from continuity and momentum equations (based on Nusselt boundary layer assumptions), are used for the numerical solution of the transport of mass and energy (respectively, eqs. 4 and 3).

$$u = \frac{\rho g}{\mu}\sin\beta\left(\delta y - \frac{1}{2}y^2\right) \tag{1}$$

$$v = -\frac{\rho g y^2}{2\mu}\left[\frac{d\delta}{dx}\sin\beta + \frac{1}{r}\left(\delta - \frac{y}{3}\right)\cos\beta\right] \tag{2}$$

$$u\frac{\partial T}{\partial x} + v\frac{\partial T}{\partial y} = a\frac{\partial^2 T}{\partial y^2} \tag{3}$$

$$u\frac{\partial \omega}{\partial x} + v\frac{\partial \omega}{\partial y} = D\frac{\partial^2 \omega}{\partial y^2} \tag{4}$$

Where the film thickness is given by eq. 5 [12].

$$\delta = \left(\frac{3\mu\Gamma}{\rho^2 g\sin\beta}\right)^{1/3} \tag{5}$$

198 The problem formulation needs to be closed by consistent initial and boundary conditions. The initial
199 conditions correspond to the solution temperature and concentration at the distributer, otherwise
200 assuming that a complete mixing occurs, to the bulk values of the previous tube.

201 At x=0 and 0<y<δ; $T=T_{in}$, $\omega=\omega_{in}$

202 The boundary conditions on the tube surface set a constant value of temperature and null diffusion.

203 At y=0; $T=T_w$, $\frac{\partial \omega}{\partial y}=0$

204 At the interface, temperature is related to interface concentration and the heat exchanger pressure
205 by the equilibrium condition.

206 At $y=\delta$; $T=T_{sat}(\omega_{if},P)$, $\omega=\omega_{if}$

207 The interface concentration is determined from Fick's law of diffusion:

208 $$G_v = -\frac{\rho D}{\omega_{if}}\frac{\partial \omega}{\partial y} \quad (6)$$

209 And the heat produced by absorption is conducted through the film towards the tube surface:

210 $$G_v i_{abs} = k\frac{\partial T}{\partial y} \quad (7)$$

211 The solution approach adopted introduces a dimensionless coordinate transformation in order to
212 map the flow domain in the physical space to a simple rectangular domain in the computational and
213 is parallel to [18]. The dimensionless variables considered in the circumferential and radial directions
214 are:

215 $$\varepsilon = \frac{x}{\pi r} = \frac{\beta}{\pi} \quad (8)$$

216 $$\eta = \frac{y}{\delta} \quad (9)$$

217 A cosine type grid is employed in the η direction to make the grid finer where steeper gradients are
218 expected, i.e. near the tube wall (η=0) surface and at the interface (η=1). First order backward

219 difference is applied for the convective term in the ε direction for both energy and species transport
220 equations. In the η direction, second order central difference scheme is used both for the first and
221 the second derivative [19], respectively belonging to the convective and diffusive terms.
222 A second order backward difference scheme is used for the first derivative of diffusion terms of the
223 boundary conditions at the interface. While, a second order forward difference is used for the first
224 derivative of concentration boundary condition at the wall.
225 The calculation is performed between $\beta=\pi/N$ and $\beta=\pi(N\text{-}1)/N$ because of the definition domain of
226 the velocity field (eq. 1 and 2).

227 ## 3. Mathematical formulation of Entropy generation

228 From the calculated temperature, velocity and concentration fields, a local irreversibility analysis of
229 water vapor absorption through a laminar, gravity driven, viscous, incompressible liquid film, flowing
230 over a cooled horizontal tube, is performed and different entropy sources are distinguished. Owing
231 to the simultaneous heat and mass transfer, four sources of irreversibility can be recognized and,
232 respectively, related to heat transfer, fluid friction, coupled effects between heat and mass transfer
233 by convection and coupled effects between heat and mass transfer by diffusion.
234 Further assumptions are required for the entropy generation mathematical formulation:

235 - Physical absorption (no chemical reactions)
236 - Steady state regime of the two dimensional flow
237 - Newtonian and incompressible, liquid film (LiBr-H_2O solution)
238 - Water vapor absorbed is considered as a perfect gas
239 - The absorption process takes place at constant pressure

240 The existence of thermal, velocity and concentration gradients in the computational field
241 representing the absorptive film yields a non-equilibrium state, which is responsible of entropy

variations (generally referred to as entropy generation). According to the problem formulation and to the introduced assumptions, the volumetric rate of entropy generation due to friction, heat and mass transfer is given by,

$$S_g = \vec{q} \cdot \vec{\nabla}\left(\frac{1}{T}\right) + \frac{\bar{\bar{\tau}} : \vec{\nabla}(V)}{T} - \frac{1}{T}\vec{j}_v \cdot \vec{\nabla}(\gamma_v) \tag{10}$$

The three terms in eq. 10 can be related, respectively, to heat transfer, fluid friction and mass transfer irreversibilities. The heat flux *q* includes the heat flux given by the Fourier Law and the enthalpy flux due to species diffusion.

$$\vec{q} = -k_S \vec{\nabla}(T) - h_v \vec{j}_v \tag{11}$$

As a result, a rearrangement of the expression gives eq.12.

$$S_g = \frac{1}{T^2} k_S \vec{\nabla}(T)^2 + \frac{1}{T^2} h_v \vec{j}_v \cdot \vec{\nabla}(T) + \frac{\bar{\bar{\tau}} : \vec{\nabla}(V)}{T} - \frac{1}{T}\vec{j}_v \cdot \vec{\nabla}(\gamma_v) \tag{12}$$

Considering the absorbed water vapor as an ideal gas and the only species diffusing through the liquid solution, its molar concentration C_v can be derived directly from the mass concentration field of LiBr (ω) resulting from the solution of energy and species transport equations.

$$C_{v,ij} = \frac{\rho_S}{M_{H_20}}(1-\omega_{ij}) - \frac{\rho_S}{M_{H_20}}(1-\omega_{in}) \tag{13}$$

The molar chemical potential of the vapor can be calculated by eq. 14, as [20].

$$\gamma_v(T, P_0) = c_{p,v}(T - T_0) - Tc_{p,v}\ln\left(\frac{T}{T_0}\right) + h_{v,0}(T_0, P_0) - Ts_{v,0}(T_0, P_0) \tag{14}$$

Where P_0 and T_0 are the standard values of pressure and temperature, respectively, 1 atm and 298 K. Standard enthalpy and entropy refer to the corresponding thermodynamic state.

The expression of vapor molar enthalpy and entropy are, respectively, given by,

$$h_v = c_{p,v}(T - T_0) + h_{v,0} \tag{15}$$

$$s_v = c_{p,v} \ln\left(\frac{T}{T_0}\right) + s_{v,0} \tag{16}$$

The shear stress is given by eq. 17.

$$\tau = \mu_S \left(\frac{\partial u}{\partial y} + \frac{\partial v}{\partial x}\right) \tag{17}$$

Thus, the local volumetric entropy generation rate can be expressed as,

$$S_g = \frac{k_S}{T^2}\left[\left(\frac{\partial T}{\partial x}\right)^2 + \left(\frac{\partial T}{\partial y}\right)^2\right] + \frac{\mu_S}{T}\left\{2\left[\left(\frac{\partial u}{\partial x}\right)^2 + \left(\frac{\partial v}{\partial y}\right)^2\right] + \left[\left(\frac{\partial u}{\partial y}\right) + \left(\frac{\partial v}{\partial x}\right)\right]^2\right\} + \\ + \frac{h_v}{T^2}\left[j_{v,x}\left(\frac{\partial T}{\partial x}\right) + j_{v,y}\left(\frac{\partial T}{\partial y}\right)\right] - \frac{1}{T}\left[j_{v,x}\left(\frac{\partial \gamma_v}{\partial x}\right) + j_{v,y}\left(\frac{\partial \gamma_v}{\partial y}\right)\right] \tag{18}$$

The transverse and axial molar fluxes are, respectively, given by,

$$j_{v,x} = C_v u - D_{vS}\frac{\partial C_v}{\partial x} \tag{19}$$

$$j_{v,y} = C_v v - D_{vS}\frac{\partial C_v}{\partial y} \tag{20}$$

By substituting the fluxes and enthalpy expressions and by calculating the derivatives of the molar chemical potential, the expression can be finally reorganized for representing the case of gas absorption into a falling liquid film.

$$S_g = \frac{k_S}{T^2}\left[\left(\frac{\partial T}{\partial x}\right)^2 + \left(\frac{\partial T}{\partial y}\right)^2\right] + \frac{\mu_S}{T}\left\{2\left[\left(\frac{\partial u}{\partial x}\right)^2 + \left(\frac{\partial v}{\partial y}\right)^2\right] + \left[\left(\frac{\partial u}{\partial y}\right) + \left(\frac{\partial v}{\partial x}\right)\right]^2\right\} + \\ + \left[c_{p,v}(T - T_0) + h_{v,0} + T\left(c_{p,v}\ln\left(\frac{T}{T_0}\right) + s_{v,0}\right)\right]\left[\frac{C_v}{T^2}\left(v\frac{\partial T}{\partial y} + u\frac{\partial T}{\partial x}\right) - \frac{D_{vS}}{T^2}\left(\frac{\partial C_v}{\partial y}\frac{\partial T}{\partial y} + \frac{\partial C_v}{\partial x}\frac{\partial T}{\partial x}\right)\right] \tag{21}$$

Different terms, related to different entropy variation sources, can be distinguished. The first term of the right-hand side of eq. 21 stands for the irreversibility due to heat transfer S_t.

$$S_t = \frac{k_S}{T^2}\left[\left(\frac{\partial T}{\partial x}\right)^2 + \left(\frac{\partial T}{\partial y}\right)^2\right] \quad (22)$$

The second term is due to fluid friction.

$$S_f = \frac{\mu_S}{T}\left\{2\left[\left(\frac{\partial u}{\partial x}\right)^2 + \left(\frac{\partial v}{\partial y}\right)^2\right] + \left[\left(\frac{\partial u}{\partial y}\right) + \left(\frac{\partial v}{\partial x}\right)\right]^2\right\} \quad (23)$$

The third and the fourth terms are related to the coupling effects between heat and mass transfer, by convection and diffusion, respectively.

$$S_c = \left[c_{p,v}(T - T_0) + h_{v,0} + T\left(c_{p,v}\ln\left(\frac{T}{T_0}\right) + s_{v,0}\right)\right]\left[\frac{C_v}{T^2}\left(v\frac{\partial T}{\partial y} + u\frac{\partial T}{\partial x}\right)\right] \quad (24)$$

$$S_d = -\left[c_{p,v}(T - T_0) + h_{v,0} + T\left(c_{p,v}\ln\left(\frac{T}{T_0}\right) + s_{v,0}\right)\right]\left[\frac{D_{vS}}{T^2}\left(\frac{\partial C_v}{\partial y}\frac{\partial T}{\partial y} + \frac{\partial C_v}{\partial x}\frac{\partial T}{\partial x}\right)\right] \quad (25)$$

The solution properties are calculated for the inlet values of temperature, pressure and concentration, with reference to [21].

4. Results

A general analysis has been carried out for typical conditions of a single absorber tube in a chiller and in a heat transformer, respectively working with coolant temperatures of 32℃ and 83℃, and outside pressure of 1.0 kPa and 12.5 kPa. The initial conditions of the LiBr-H_2O solution film have been set at the equilibrium temperature for a 60% concentration solution at the absorber vapour pressure. Furthermore, the variation of mass flow rate due to absorption of water vapor is considered negligible. This assumption is valid for a mass flow-rate higher than 0.001kg·$m^{-1}s^{-1}$, and accordingly, this analysis has been performed in a consistent mass flow-rate range [20]. Since Nusselt integral solution for velocity distribution is not defined at the inlet and outlet positions, respectively ε=0 and

ε=1, the total entropy generation S_G has been evaluated between ε=1/N and ε=N-1/N inside the whole film thickness.

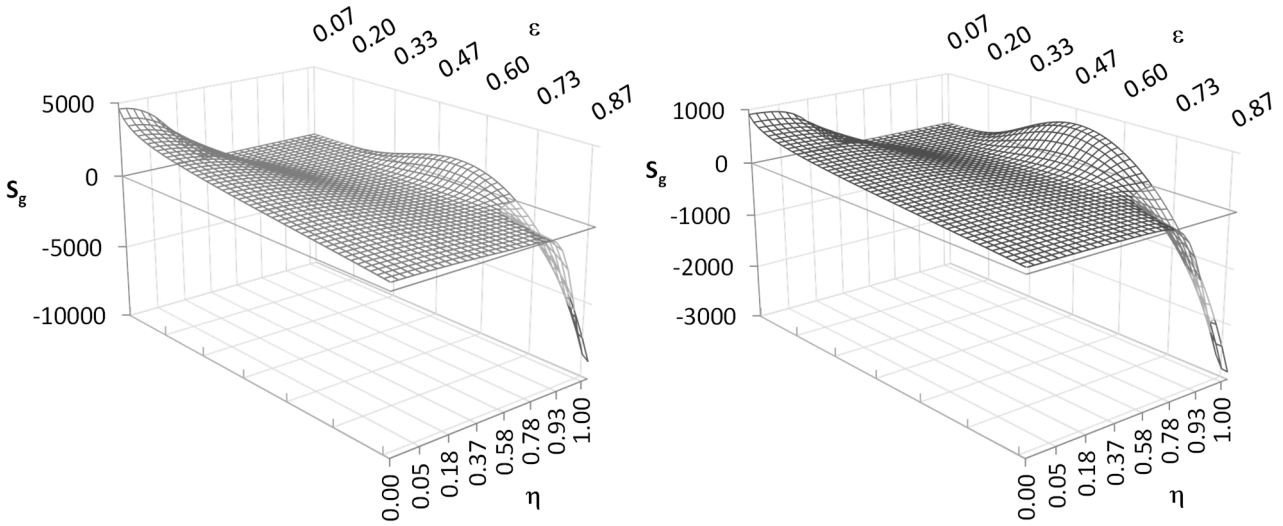

(a) (b)

Figure 2 Local entropy generation rate [kW·m^{-3}K^{-1}]; m=0.045 kg·m^{-1}s^{-1}, ω_{in}=60%, (a) T_{in}=46.6℃, P=1kPa, T_w=32℃, (b) T_{in}=97.1℃, P=12.5kPa, T_w=83℃, flowing over a tube with outer radius r=8mm.

The total entropy generation rate per unit volume S_g for an absorptive LiBr-H_2O solution flowing on a cooled horizontal tube is illustrated in Figure 2 as the superimposition of the different groups previously identified. S_g shows a local minimum in the radial direction except in the first and the last parts of the tube surface, where the total entropy generation rate is relentlessly decreasing from the wall to the film interface. The minimum is determined by the contemporaneity of wall heat transfer, friction and coupled heat and mass transfer at the interface, and it is positioned at the penetration distance of the diffusing vapor inside the film. In the second half of the tube surface the total entropy generation rate S_g at the film interface assumes negative values, due to the only negative contribution of the group related to the coupled effects of mass convection and heat transfer S_c: this behaviour can be explained considering that the local temperature decreases in the stream-wise

311 direction and vapor concentration C_v increases in that region (eq. 24, where the term $C_v u/T^2 \cdot \partial T/\partial x$ is
312 dominant).
313 In order to compare the performance of the system with the actual amount of irreversibility
314 introduced, the local volumetric entropy generation rate is integrated over the film physical domain.
315 Considering film thickness and the circumference of the tube the entropy generation per unit length
316 of the tube E is defined by eq. 26.

317 $$E = 2\int_0^{\pi r}\int_0^{\delta} S dy dx \tag{26}$$

318 The parametric analysis performed ascertains that a minimum entropy generation can always be
319 identified in terms of the film Reynolds number (defined by eq. 27), which establishes the optimal
320 thermodynamic condition in terms of entropy generation rate per unit length (Figure 3). As previously
321 stated, in this work by "optimum" the least irreversible operating condition for a specified objective
322 is meant, or otherwise, the most desirable trade-off between two or more competing irreversibilities
323 [1]. Entropy generation minimization had been also applied to design counter-flow heat exchangers
324 [22], [23], [24] or desiccant systems [25], [26], [27], [28].

325 $$\mathrm{Re} = \frac{4\Gamma}{\mu} \tag{27}$$

326 In general, higher temperature applications have lower entropy generation and cope with higher
327 solution Reynolds. The general trend of the different groups can be examined in Figure 3. Increasing
328 Reynolds numbers determine increasing friction and decreasing absorption rates, and their
329 respective entropy generation groups (E_f and E_d) show consistent trends. The combined effects of
330 increasing extension of the entrance region, increasing film thickness and decreasing absorption heat
331 release, globally establish an increasing behaviour of the thermal related irreversibilities E_t. The
332 entropy generation group related to the coupled effects of mass convection and heat transfer E_c

shows a local minimum (maximum of the absolute value), which can be explained considering that when Reynolds number is increased convection is amplified while absorption heat release is reduced. As already pointed out regarding the corresponding term of volumetric entropy generation, this group assumes negative values.

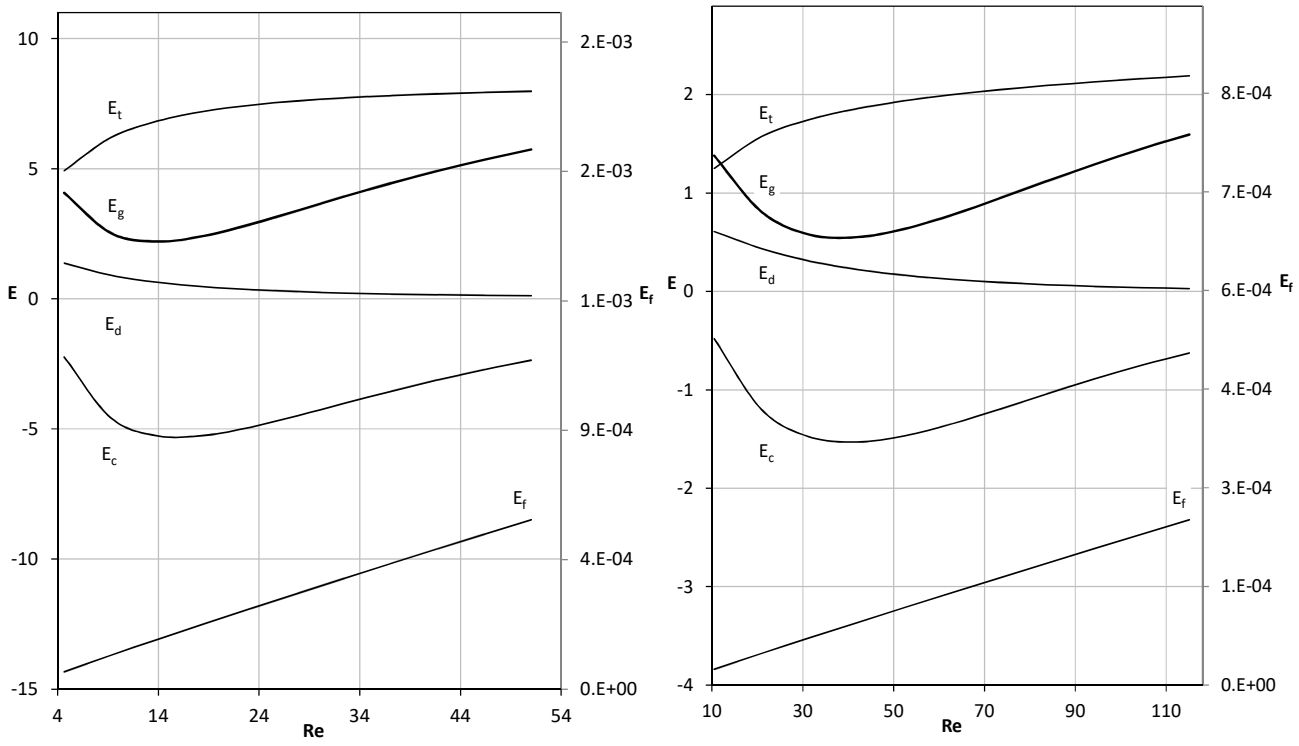

Figure 3 Various entropy generation groups per unit length of the tube [W·m^{-1}K^{-1}] as a function of film Reynolds number; (a) T_w=32℃, ω_{in}=60%, T_{in}=46.6℃, P=1kPa, (b) T_w=83℃, ω_{in}=60%, T_{in}=97.1℃, P=12.5kPa

Absorber design and operability parameters can be considered in the analysis. A graphical parametric study is performed evaluating the influence on the entropy generation rate of a different tube radius, coolant inlet temperature and inlet solution temperature as function of the film Reynolds number. At first, equilibrium of the inlet solution with respect to the vapour temperature (and pressure) is considered.

The influence of the radius on the global entropy generation and on each entropy generation group as a function of solution mass flow rate (e.g. Reynolds Number, defined by eq. 27), for fixed inlet and boundary conditions is presented, respectively, in Figure 4 and Figure 5. As a rule, lower tube radii present lower entropy generation rates per unit length and match with lower solution Reynolds values (Figure 4). The trend of the global entropy generation shows a minimum value and the corresponding Reynolds number could be considered as a least irreversibility operative condition. For the chiller application case (Figure 4a), least irreversibility Reynolds numbers of 10, 14 and 23 are obtained, respectively, for tube radii of 5, 8 and 11mm. For the same values of tube radii, but for an absorber operating at reference conditions for a heat transformer, the least irreversibility Reynolds numbers are, respectively, 31, 42 and 52 (Figure 4b). These values have been obtained without considering partial wetting of the exchange surface, but usually they correspond to solution mass flow rates which are not able to assure complete wetting, unless tension-active surfactants are added to the solution.

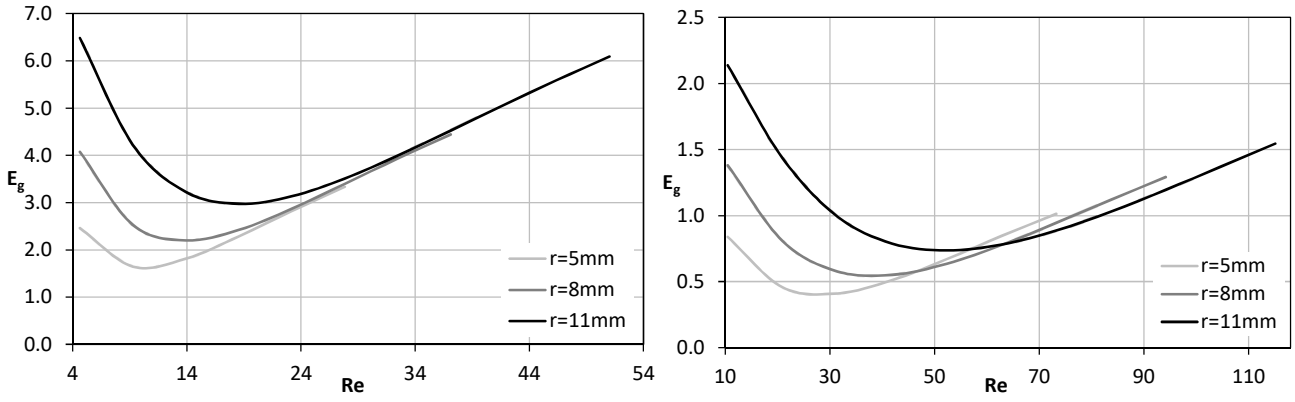

(a) (b)

Figure 4 Entropy generation rate per unit length [$W \cdot m^{-1}K^{-1}$] as a function of Reynolds number for different values of the tube radius; (a) T_w=32℃, ω_{in}=60%, T_{in}=46.6℃, P=1kPa, (b) T_w=83℃, ω_{in}=60%, T_{in}=97.1℃, P=12.5kPa

Figures 5(a-b) show the effect of different tube radii on each entropy generation group. A bigger radius increases the absolute value of every entropy generation group. In fact, when entropy generation is integrated over the film thickness and the tube circumference the group related to thermal irreversibility E_t shows a relaxingly-increasing trend with respect to Reynolds number. Contrarily, the vapor diffusion related irreversibility E_d is characterised by a relentlessly decreasing trend. The group related to the coupled effects of mass convection and heat transfer E_c has a critical influence on the global trend of the entropy generation rate per unit length E_g and, as already pointed out, it shows a local minimum, which can be explained considering that, increasing Reynolds number, the velocity field is intensified while absorption heat release is reduced. A greater outer radius moves the minimum to higher *Re* and to lower values of E_c. Finally, the greater the tube radius the higher the friction related irreversibility E_f.

Comparing chiller and heat transformer applications, as a rule, the first corresponds to higher entropy generation rate and the latter highlights a greater impact of the diffusion related irreversibility.

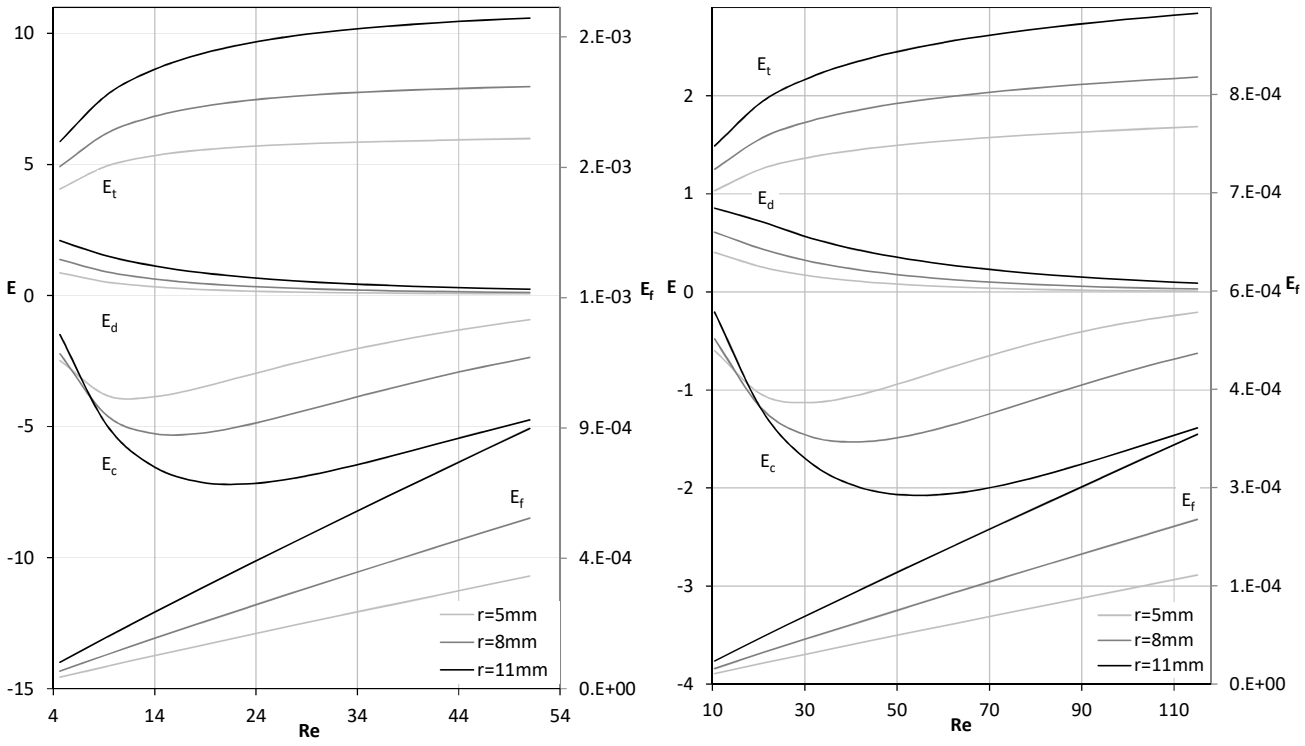

(a) (b)

Figure 5 Effect of different radii on the various entropy generation groups [$W \cdot m^{-1}K^{-1}$]; (a) T_w=32℃, ω_{in}=60%, T_{in}=46.6℃, P=1kPa, (b) T_w=83℃, ω_{in}=60%, T_{in}=97.1℃, P=12.5kPa

In general, a lower tube wall temperature increases heat transfer and, increasing the driving force for vapor absorption, mass transfer at the interface. Accordingly, Figure 6 makes evidence of a higher entropy generation when tube wall temperature is decreased, while the optimal Reynolds is weakly dependent on this parameter.

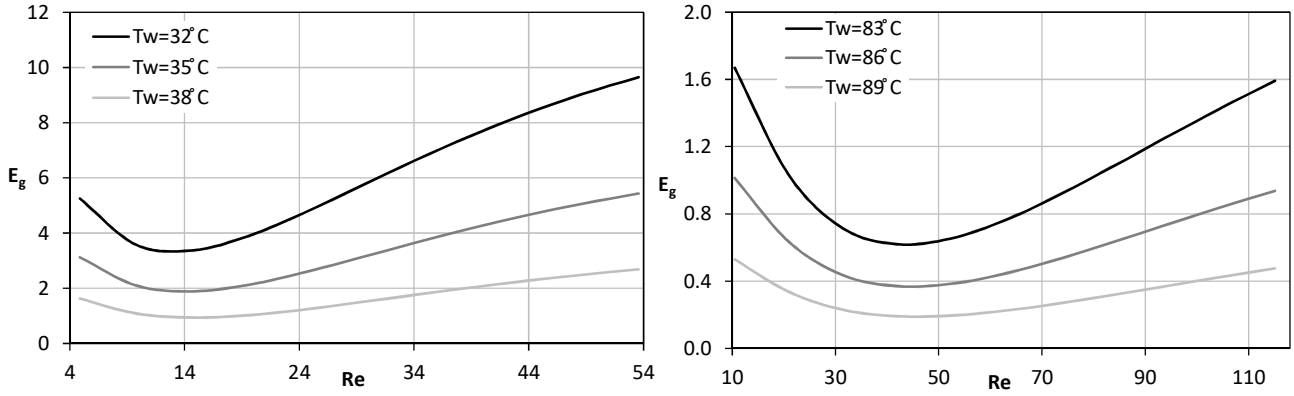

(a) (b)

Figure 6 Entropy generation rate per unit length [$W \cdot m^{-1}K^{-1}$] as a function of Reynolds number for different values of the tube wall temperature; (a) r=9mm, ω_{in}=60%, T_{in}=46.6℃, P=1kPa, (b) r=9mm, ω_{in}=60%, T_{in}=97.1℃, P=12.5kPa

Figures 7(a-b) describe the effect of different tube wall temperatures on the various entropy generation group. A lower wall temperature increases temperature gradients and, once the temperature gradient reaches the interface, also concentration gradients. Also friction related irreversibility E_f (eq. 23) is affected indirectly by a different wall temperature which determines a different temperature field.

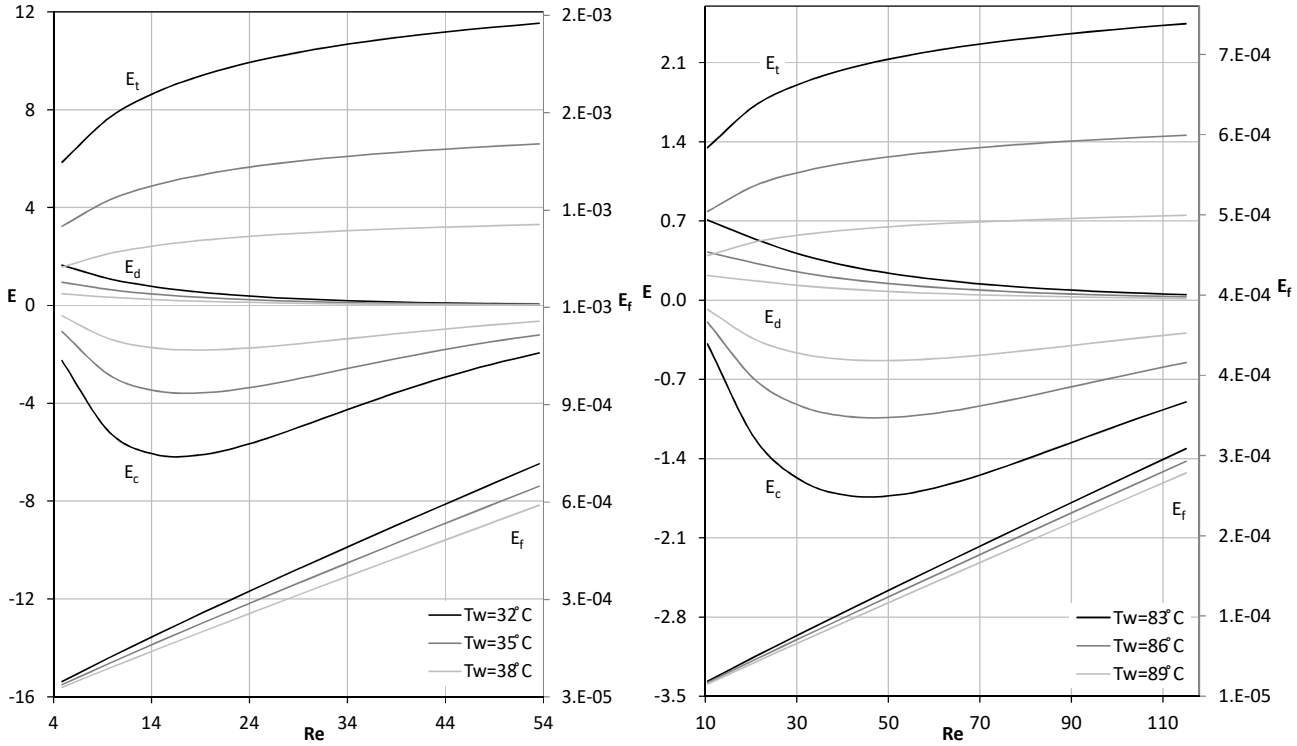

(a) (b)

Figure 7 Effect of different wall temperatures on the various entropy generation groups [$W \cdot m^{-1}K^{-1}$]; (a) r=9mm, ω_{in}=60%, T_{in}=46.6℃, P=1kPa, (b) r=9mm, ω_{in}=60%, T_{in}=97.1℃, P=12.5kPa

Furthermore, in order to analyse the effect of a different equilibrium temperature at the interface (and, due to the equilibrium hypothesis, a different absorber pressure), the calculations are extended aver a range of different inlet solution temperatures for both the chiller and the heat transformer applications. Since the tube wall temperature is maintained constant, different inlet temperatures have a similar effect to that of different wall temperatures for a fixed inlet condition. However, for the same temperature difference T_i-T_w, a change in the inlet temperature value brings about a smaller entropy generation than that correspondingly obtained by changing the wall temperature. Also, lower the inlet temperatures are associated to slightly lower Reynolds corresponding to the optimal condition (Figure 8).

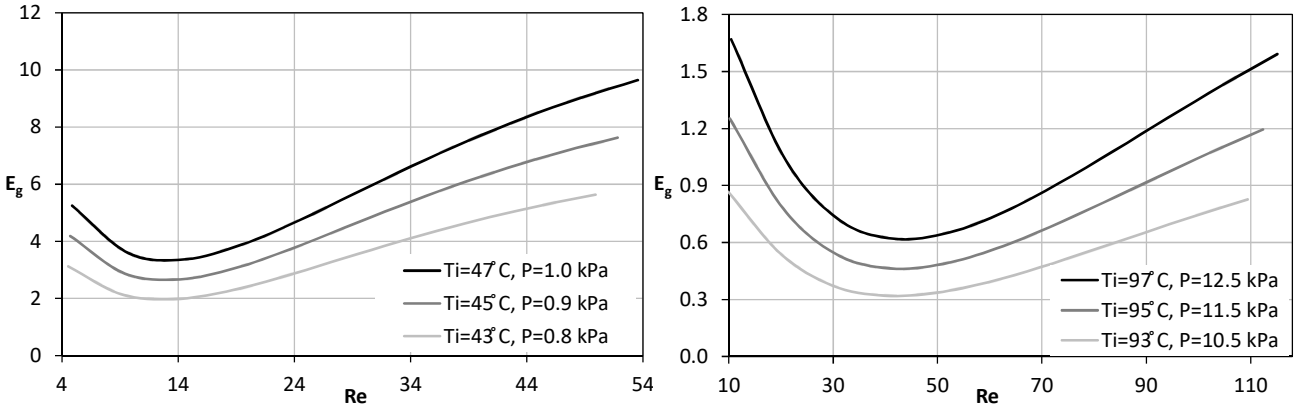

(a) (b)

Figure 8 Entropy generation per unit length [W·m^{-1}K^{-1}] as a function of Reynolds number for different inlet temperatures; (a) r=9mm, ω_{in}=60%, T_w=32℃, (b) r=9mm, ω_{in}=60%, T_w=83℃

Acting again on the temperature difference T_i-T_w, inlet solution temperature variations have similar effects to those of a different wall temperature on the entropy generation groups as function of film Reynolds number and the corresponding graph is omitted.

5. Heat and mass transfer optimization

As a rule, the formulation of thermodynamic optimization criteria has always accompanied the analysis of energy systems in order to improve their performance. Since the development of finite-time thermodynamics, the attention has been moved towards the concept of non-equilibrium processes and their related irreversibility sources. The use of absorption systems has attracted a remarkable attention and shown a great potential in the utilization of low-grade heat sources [29] [30] [31] [32]. Both chiller and heat transformer configurations have been generally analysed from a first and second principle point of view [33] [34] [35] [36] [37] [38]. Based on the previous thermodynamic analysis of the irreversibility associated to the absorption of vapour and the heat transfer in a falling film configuration of the absorber, this paper aims at the definition of proper dimensionless parameters for the optimization of this component regarding the ultimate duty of the

system. In general, a heat transformer is a device which aims at delivering heat at a higher temperature than the given temperature of the heat source. The component of the plant which actuates this final heat transfer is the absorber. Absorption refrigeration machines are supposed to extract heat at a lower temperature than those of the ambient and the driving-fluid in the generator. The cooling effect is realized by the evaporation of the condensed refrigerant, which is then absorbed by the solution inside the absorber, in order to be effectively pumped at the generator pressure level and start the cycle again. Accordingly, the best thermodynamic condition of the absorber operability in the two application cases considered corresponds to two different conditions.

For the first principle of thermodynamics, the COP of an absorption system can be expressed in a general way by eq. 28 for a refrigeration application and eq. 29 in case of heat boosting one.

$$COP_{CH} = \frac{Q_E}{L}\frac{L}{Q_G} = \frac{Q_E}{Q_C - Q_E}\frac{Q_G - Q_A}{Q_G} = \frac{Q_E}{T_C\left(\frac{Q_C}{T_C} - \frac{Q_E}{T_C}\right)}\frac{T_A\left(\frac{Q_G}{T_A} - \frac{Q_A}{T_A}\right)}{Q_G} \tag{28}$$

$$COP_{HT} = \frac{Q_A}{L}\frac{L}{Q_G} = \frac{Q_A}{Q_A - Q_E}\frac{Q_G - Q_C}{Q_G} = \frac{Q_A}{T_E\left(\frac{Q_A}{T_E} - \frac{Q_E}{T_E}\right)}\frac{T_C\left(\frac{Q_G}{T_C} - \frac{Q_C}{T_C}\right)}{Q_G} \tag{29}$$

Introducing the second principle of thermodynamics, applied to irreversible cycles where isothermal heat transfer without any temperature difference at the heat exchange occurs, is possible to state,

$$\frac{Q_C}{T_C} = \frac{Q_E}{T_E} + \sigma_{EC} \quad , \quad \frac{Q_A}{T_A} = \frac{Q_G}{T_G} + \sigma_{GA} \tag{30}$$

$$\frac{Q_A}{T_A} = \frac{Q_E}{T_E} + \sigma_{EA} \rightarrow \frac{Q_E}{T_E} = \frac{Q_A}{T_A} - \sigma_{EA} \quad , \quad \frac{Q_C}{T_C} = \frac{Q_G}{T_G} + \sigma_{GC} \tag{31}$$

Accordingly, the expression of the system performance in terms of COP can be rearranged highlighting the influence of components irreversibility.

445 $$COP_{CH} = \frac{Q_E}{T_C\left(\frac{Q_E}{T_E} + \sigma_{EC} - \frac{Q_E}{T_C}\right)} \frac{T_A\left(\frac{Q_G}{T_A} - \frac{Q_G}{T_G} - \sigma_{GA}\right)}{Q_G} = \frac{1 - \frac{T_A}{T_G} - \frac{\sigma_{GA}T_A}{Q_G}}{\frac{T_C}{T_E} - 1 + \frac{\sigma_{EC}T_C}{Q_E}} = \frac{\eta_{CaTM-GA} - \frac{\sigma_{GA}T_A}{Q_G}}{\frac{1}{\eta_{CaRM-EC}} + \frac{\sigma_{EC}T_C}{Q_E}} \quad (32)$$

446 $$COP_{HT} = \frac{Q_A}{T_E\left(\frac{Q_A}{T_E} - \frac{Q_A}{T_A} + \sigma_{EA}\right)} \frac{T_C\left(\frac{Q_G}{T_C} - \frac{Q_G}{T_G} - \sigma_{GC}\right)}{Q_G} = \frac{1 - \frac{T_C}{T_G} - \frac{\sigma_{GC}T_C}{Q_G}}{1 - \frac{T_E}{T_A} + \frac{\sigma_{EA}T_E}{Q_A}} = \frac{\eta_{CaTM-GC} - \frac{\sigma_{GC}T_C}{Q_G}}{\frac{1}{\eta_{CaHP-EA}} + \frac{\sigma_{EA}T_E}{Q_A}} \quad (33)$$

447 Broadly speaking, adopting a comprehensive point of view for chiller and heat transformer
448 application cases, eq. 32 and 33 highlight the effect of irreversibility on the system performance. They
449 make evidence of the importance to minimize component irreversibility, or more precisely, they
450 states that by maximizing the dimensionless groups "Q/σT" the efficiency of the system is improved.
451 Even though the expressions obtained for the system performance are based on a simplified
452 approach, they make evidence of a dimensionless group, related to the irreversibilities, that indicate
453 a way to improve the system performance by acting also on a single device (in this case the absorber
454 of the absorption system). In a chiller or heat pump application case, the optimal performance can
455 be identified by the condition at which the absorber operates at the maximum absorption rate with
456 the least thermal power to be rejected. On the other hand, for a heat transformer, the best operative
457 condition corresponds to the maximum thermal power supplied at high temperature for the least
458 power supplied at the generator. Under this approach, based on the previous dimensionless group,
459 two different dimensionless parameters are introduced for the absorber with respect to the
460 operability of the absorption system. Eq. 34 defines the absorber dimensionless parameter used to
461 maximise heat transfer at the wall with regards to the irreversibility introduced, useful in order to
462 maximize the efficiency of the whole system in a heat transformer application.

463 $$DQ = \frac{q_W}{E_g T_W} \quad (34)$$

By maximizing the parameter *DQ* the thermal flux per unit length of the tube is maximized for a certain entropy generation inside the falling film. From a different point of view, at the maximum *DQ*, the product of the total irreversibility per unit length of the tube and the wall temperature is minimized for a certain thermal power per unit length q_W to the cooling water. The product $E_g T_W$ embodies the thermal flux associated to the entropy variation of the whole process, in case this would be generated by heat transfer at constant temperature T_W and represents the loss of available thermal power because of the process irreversibility.

Similarly, eq. 35 defines the absorber dimensionless group used to maximise absorption at the interface with regards to the irreversibility introduced, useful in order to maximize efficiency of the absorption system in chiller application.

$$DA = \frac{\Lambda i_{abs}}{E_g T_e} \tag{35}$$

T_e is the equilibrium temperature of the solution at concentration ω_{in} (under the assumption of thermodynamic equilibrium and constant concentration at the inlet T_e=T_{in}) and its physical significance corresponds to the temperature that would be reached if thermodynamic equilibrium could be obtained without changes in concentration. *DA* is the ratio between the entropy generation rate that would be produced by the heat transfer of the thermal power per unit length related to the release of the heat of absorption by the absorbed vapor at the film interface (at fixed temperature T_e) and the global entropy generation rate per unit length E_g. Defined in this way, *DA* is proportional to the $Q/\sigma T$ group appearing in eq. 32. As a result, by maximizing this parameter the absorbed vapor flux per unit length of the tube Λ (and consequently Q_E=$Z\Lambda$(i_{Eout}-i_{Ein})) is maximized for a certain entropy generation inside the falling film. Otherwise, at the maximum *DA*, the group $E_g T_e \cdot i_{abs}^{-1}$ is minimized for a certain vapor flux per unit length of the tube. This group represents the absorbed vapor flux per unit length of the tube associated to the entropy variation of the whole process, in

case this would have been generated by the release of the heat of absorption i_{abs} at constant temperature T_e.

With respect to the dimensionless parameters introduced, the operability of the absorber can be investigated and then optimized, respectively, for the absorption chiller and the heat transformer application cases under analysis.

5.1 Chiller

A single value of film Reynolds number which maximizes the dimensionless group $Q/\sigma T$ (DA for the chiller application, DQ for the heat transformer application) can always be identified. It can be highlighted that the Reynolds at which this occurs (referred to as optimum Reynolds in the following) is mainly dependent on the outer tube radius and on the application case (i.e chiller or heat transformer operability), while a weak influence of the temperature difference between the inlet solution and the wall temperature is shown (Figures 9 and 10). According to this criterion, optimal Reynolds number of 9, 13 and 16 correspond, respectively, to tube radii equal to 5mm, 8mm and 11mm for the chiller application case (Figure 9b). In general, the maximum value of DA is approximately constant and the film Reynolds that maximise mass transfer, with regard to DA, increases continuously when the tube radius is increased (Figure 9a). Indeed, it can also be stated that, for any fixed Reynolds there is an optimal value of the tube radius, whose value increases with Reynolds, but more steeply at low than high values. Accordingly it is possible to identify an asymptotic maximum value of the radius, above which is not convenient to operate with any mass flow rate.

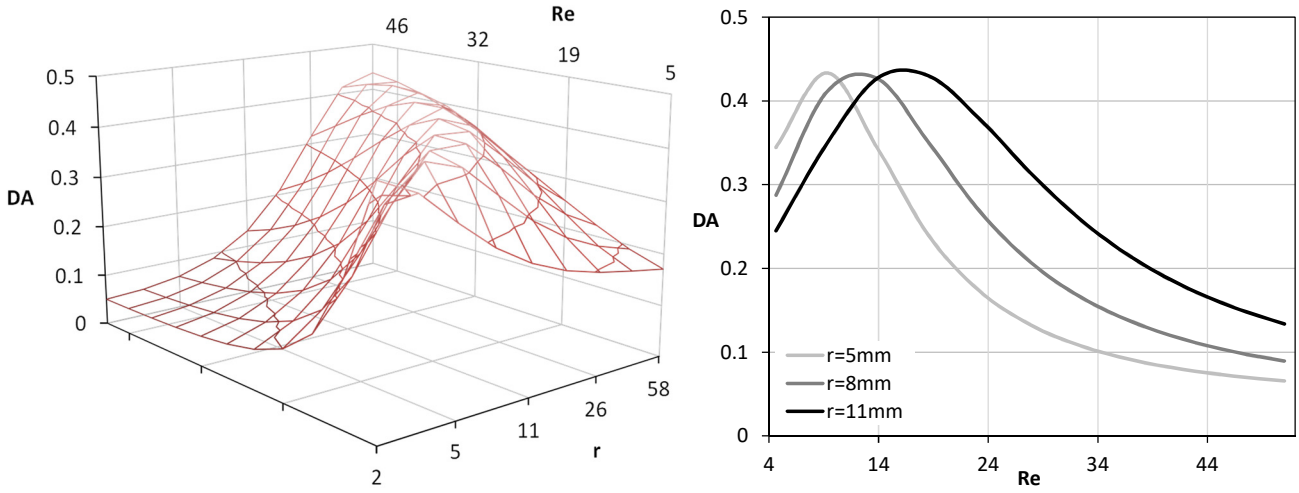

(a) (b)

Figure 9 Dimensionless parameters DA as a function of film Reynolds number for different tube radii [mm] at chiller representative conditions; ω_{in}=60%, T_{in}=46.6°C, T_w=32℃, P=1kPa (T_e=46.6°C)

On the other hand, when the difference between inlet and wall temperature is decreased (by increasing the tube wall temperature, i.e. the cooling water temperature, or decreasing the solution inlet temperature), for a fixed Reynolds, the dimensionless group *DA* defined show a persistently increasing trend (Figure 10a). This behaviour can be explained considering the fact that a lower temperature of the tube wall increases heat transfer (and indirectly mass transfer), but, at the same time, the irreversibility associated to the absorption process increases at a higher rate. However, an optimal condition in terms of film Reynolds number can always be identified and the corresponding value increases with increasing inlet temperatures of the solution. In particular, optimal Reynolds number of 8, 9 and 11 correspond, respectively, to inlet temperatures equal to 43℃, 45℃ and 47℃ for the chiller application case (Figure 10b).

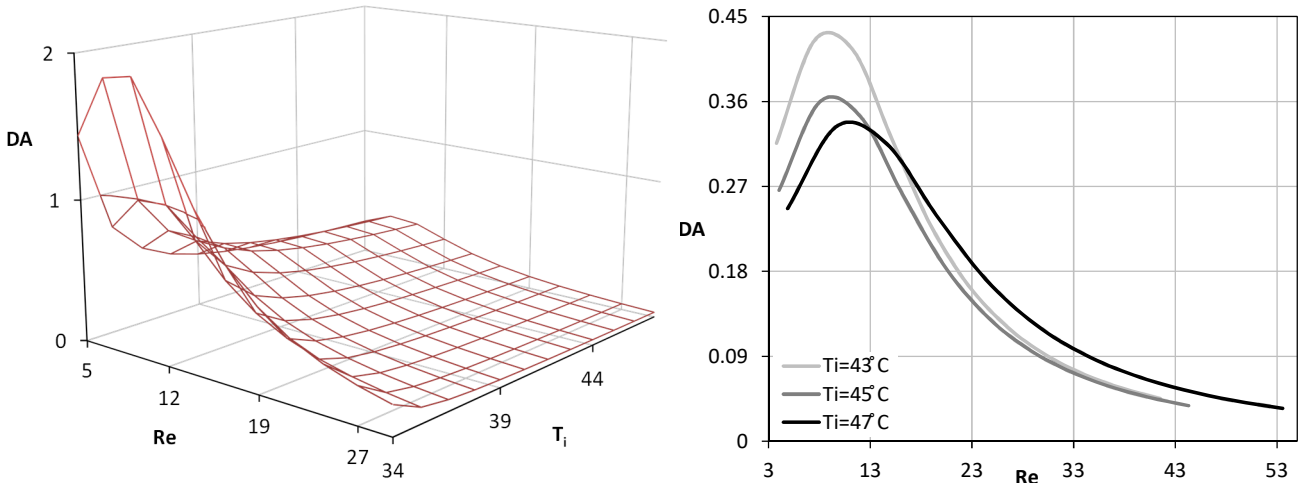

(a) (b)

Figure 10 Dimensionless parameters DA as a function of film Reynolds number for various inlet solution temperatures at chiller representative conditions; r=9mm, ω_{in}=60%, T_w=32.0℃

The previous calculation has been performed under the assumption of thermodynamic equilibrium between the inlet solution and the vapor at the absorber pressure. However, this condition, which is suitable for a general irreversibility analysis, doesn't usually correspond to the operability of the absorber in actual plants [10]. Accordingly, relaxing this hypothesis, the analysis is extended to conditions which are characterised by the sub-cooling of the inlet solution through the definition of the dimensionless parameter θ. The latter (eq. 36) expresses the temperature-boundary and initial conditions in a dimensionless form, linking the sub-cooling of the solution to the temperature difference between the wall and the equilibrium temperature of the inlet solution with the vapour at the absorber pressure.

$$\theta = \frac{T_e - T_{in}}{T_{in} - T_W} \tag{36}$$

In general, by introducing a 2℃ sub-cooling of the solution and keeping it constant, the maximum values of *DA* move to higher Reynolds (Figure 11). The behaviour of the objective function *DA* with respect to Reynolds and the tube outer radius in the case of a sub-cooled solution is qualitatively and

quantitatively similar to the case of an inlet solution at thermodynamic equilibrium with the vapor in the absorber (Figure 9).

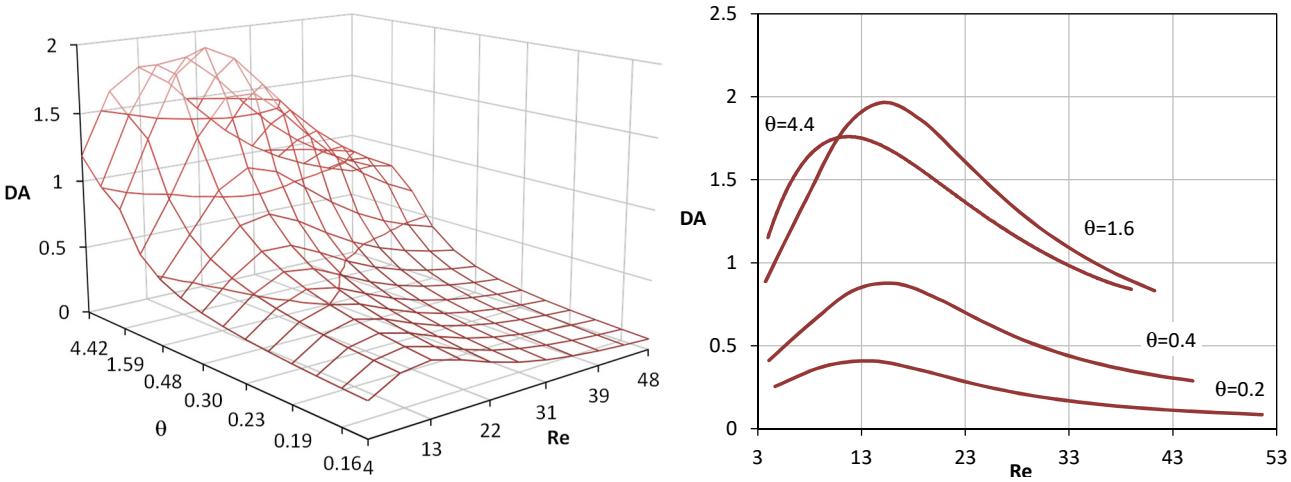

(a) (b)

Figure 11 Dimensionless parameters DA as a function of film Reynolds number and inlet temperature at chiller representative conditions, 2°C sub-cooling inlet solution, r=9mm, ω_{in}=60%, T_w=32.0℃, P=1kPa

In order to investigate the influence of the sub-cooling, it is then possible to change the θ value keeping fixed T_w and T_e value (Figure 12). Higher values of the sub-cooling at the inlet move the maximum to higher Reynolds. Assuming a different standpoint in the optimization of the absorber in a chiller absorption system, we can say that a best value of the solution sub-cooling (i.e. θ) can be identified when both T_w and T_e are fixed and furthermore, for a fixed value of θ, an optimal Reynolds can always be identified, and, reversely, for a fixed Reynolds an optimal θ can be established. What is more, when the absorber works with an inlet solution characterized by the optimal value of the sub-cooling, the corresponding optimal Reynolds is maximized (Re=17). This approach suggests again operating at low solution mass flow rates and with a small temperature difference between the inlet solution and the cooling water. Consistently, in the specific case of falling film heat exchangers, the film thickness constitutes the main heat transfer resistance with the cooling water circulating inside

555 the tube and it has been theoretically and experimentally recognized that working with reduced
556 solution mass flow rate can improve the system performance. As a result, operability at reduced
557 Reynolds number is attractive for absorption plants, but the tube partial wetting at low solution flow
558 rate needs to be considered as a critical related issue. Regarding the temperature difference between
559 the inlet solution and the cooling water (directly related to the tube wall temperature T_w), a low value
560 of this parameter reduces the irreversibility of the process. However, under this point of view in a
561 specific application case the size constraint of the system is expected to be decisive.

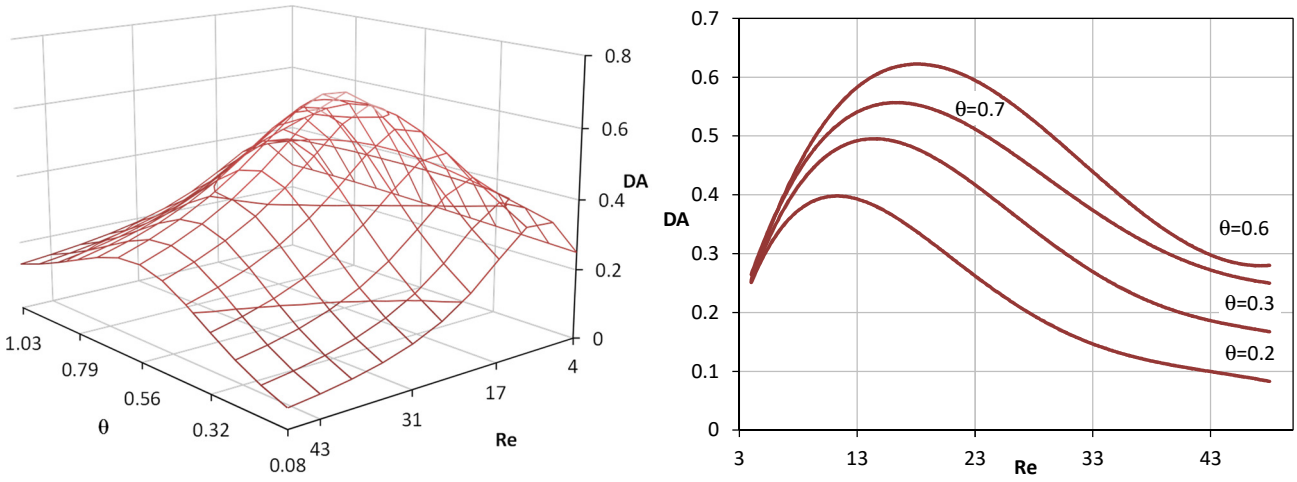

562

563 (a) (b)

564 **Figure 12 Dimensionless parameters DA as a function of film Reynolds number and solution sub-**
565 **cooling at chiller representative conditions, r=9mm, ω_{in}=60%, T_w=32.0℃, T_e=46.6℃, P=1kPa**

566 Both Figures 11 and 12 show a maximum of the *DA* value. By considering the physical meaning of this
567 parameter from a system point of view, the chiller (or the heat pump) operates at the maximum
568 absorption rate with the least irreversibility introduced by the absorber, and, bearing in mind eq. 32,
569 this is beneficial to the whole system COP.

570 ### 5.2 Heat transformer

571 Similarly to the absorption chiller case, the absorber of an absorption heat transformer is studied by
572 means of an analysis of the dimensionless group *DQ* defined by Eq. 34. Firstly, thermodynamic

equilibrium between the inlet solution and the absorbed vapor is assumed. Figures 13 shows that the maximum value of *DQ* is roughly constant, but for increasing tube radii, the optimal Reynolds number increases as well. According to this criterion, for the heat transformer application case, Reynolds number of 30, 40 and 55 maximize heat transfer in the absorber (or minimize the process irreversibility), respectively, when the tube radii are equal to 5mm, 8mm and 11mm.

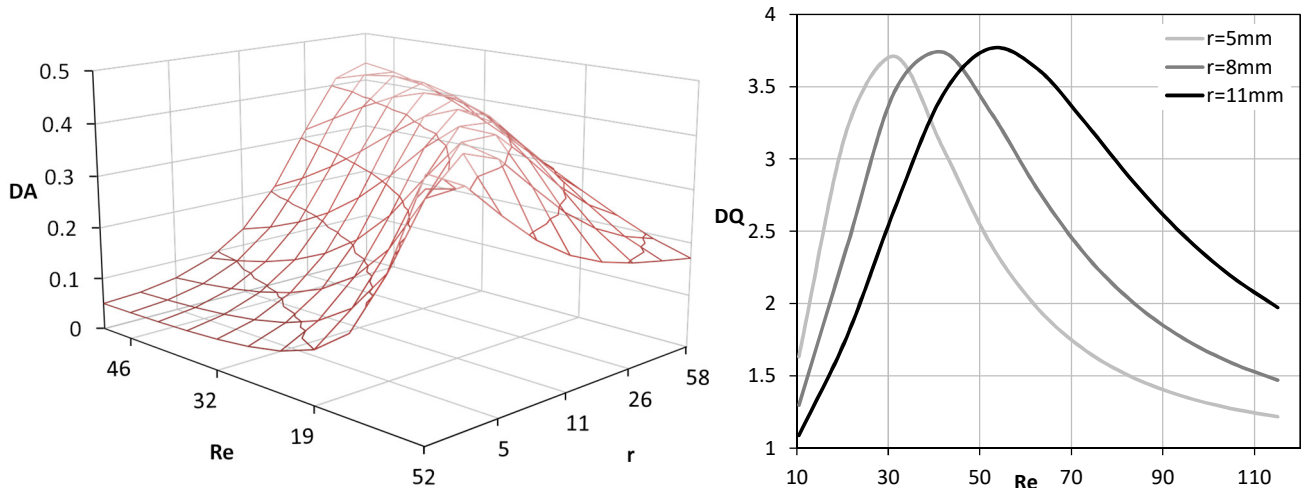

(a) (b)

Figure 13 Dimensionless parameters DQ as a function of film Reynolds number and tube outer radius [mm] at heat transformer representative conditions, T_w=83.0℃, ω_{in}=60%, T_{in}=97.1℃, P=12.5kPa

Similarly to *DA*, the maximum value of *DQ* is roughly constant, but for increasing tube radii, the optimal Reynolds number increases as well (Figure 13). According to this criterion, for the heat transformer application case, Reynolds number of 30, 40 and 55 maximise heat transfer in the absorber (or minimize the process irreversibility), respectively, when the tube radii equal to 5mm, 8mm and 11mm. Moreover, the value of Reynolds which maximizes *DQ* is weakly influenced by the temperature difference between the inlet and the wall temperature, as shown in Figure 14 for different wall temperatures. *DQ* increases relentlessly when the wall temperature is augmented (i.e.

the temperature difference between the inlet solution value and the wall is lowered) for a fixed Reynolds number (Figure 14a).

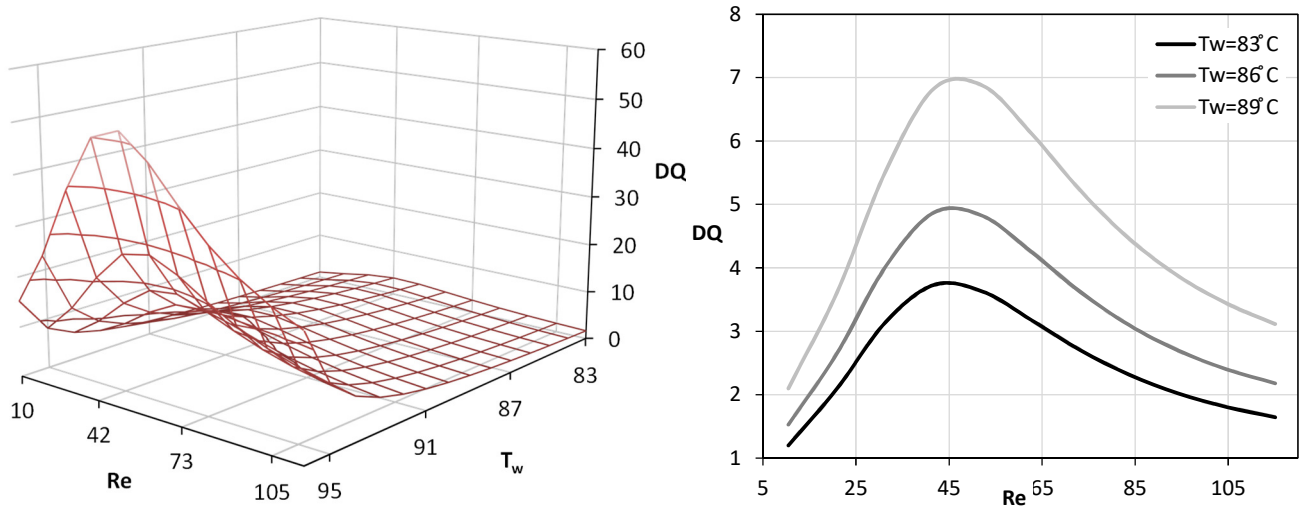

(a) (b)

Figure 14 Dimensionless parameters DQ as a function of film Reynolds number and tube wall temperature at heat transformer representative conditions, r=9mm, ω_{in}=60%, T_{in}=97.1℃, P=12.5kPa

When the assumption of thermodynamic equilibrium of the inlet solution is relaxed and a 2℃ sub-cooling is introduced consistently with the calculation performed for the chiller application, the maxima move to slightly higher Reynolds (Figure 15). Also, the influence of the wall temperature is intensified and higher T_w are associated to increasing Reynolds. More significantly, an optimal *DQ* condition can be shown with respect to T_w and Reynolds for the heat transformer; 0.035kg·m^{-1}s^{-1}, T_w=92℃ (Figure 15a). In this circumstance the optimal wall temperature is minimized and the optimal Reynolds is maximized (Re=71). The behaviour of the previously defined objective function *DQ* with respect to Reynolds and the tube outer radius for a sub-cooled solution is similar to the case of an inlet solution at thermodynamic equilibrium with the vapor in the absorber, hence, is not represented herein.

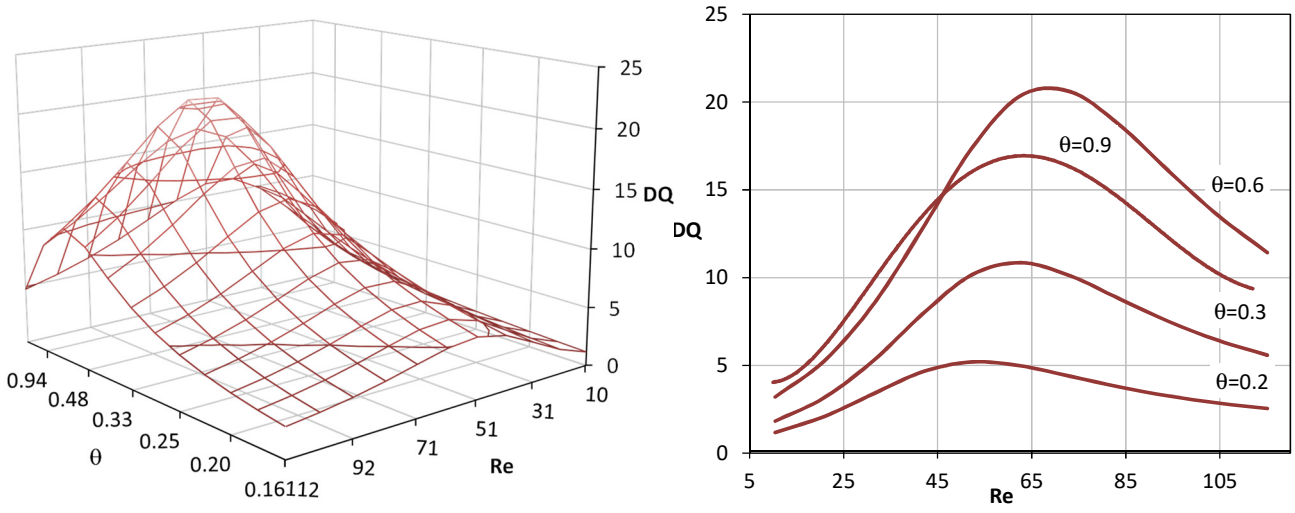

(a) (b)

Figure 15 Dimensionless parameters DQ as a function of film Reynolds number and tube wall temperature at heat transformer representative conditions, 2°C sub-cooling inlet solution, r=9mm, ω_{in}=60%, T_{in}=95.1℃, P=12.5kPa

When both T_w and T_e are fixed and the sub-cooling of the inlet solution becomes a parameter, a best value of the latter can be identified (Figure 16). Up to that value, higher sub-cooling at the inlet move the optimal condition to lower wall temperatures and higher Reynolds. By referring to the physical meaning of this parameter and the different operability of the absorber in the heat transformer application case considered, while maximising *DQ*, ceteris paribus for the operative conditions other than the absorber, the whole systems operate at its highest COP and best thermodynamic state. This condition corresponds to the maximum thermal power supplied by the heat transformer at high temperature for the least irreversibility introduced by the absorber.

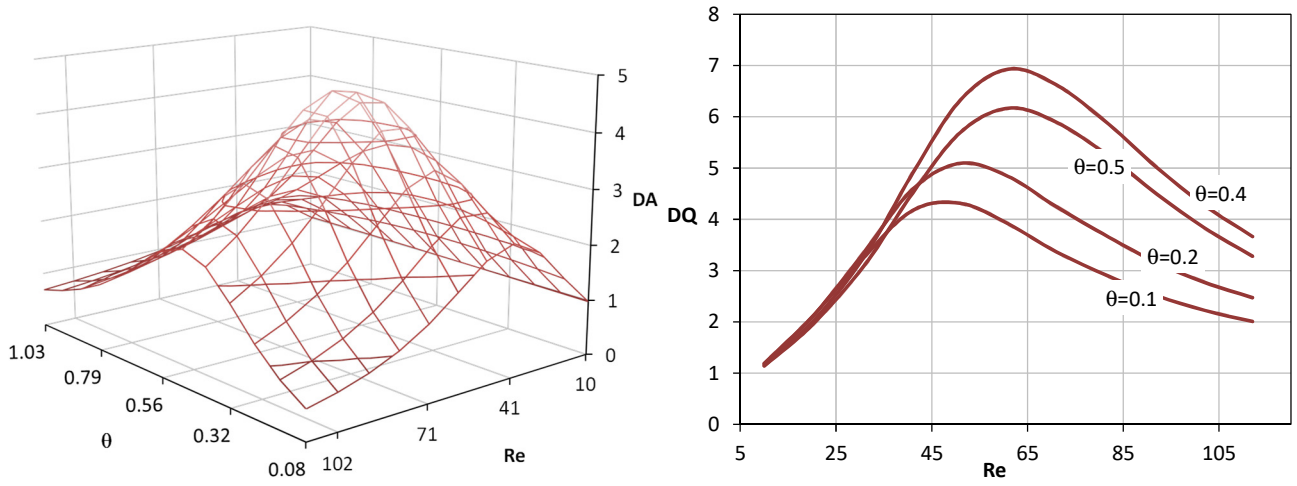

620

621 **Figure 16 Dimensionless parameters DQ as a function of film Reynolds number and solution sub-**

622 **cooling at heat transformer representative conditions, r=9mm, ω_{in}=60%, T_w=83.0℃, T_e=97.1℃,**

623 **P=12.5kPa**

624 ## 5. Conclusions

625 The LiBr-H_2O concentration and temperature distribution inside the laminar falling film have been
626 obtained from the numerical solution of the coupled system of species and energy transport
627 equations. Velocity, temperature and concentration fields, in turn, allow estimating the gradients
628 and fluxes of these variables and, finally, the local volumetric entropy generation of an absorptive
629 film flowing over a cooled horizontal tube. From the general expression obtained, various entropy
630 generation groups, distinguished in regard to different entropy variations sources, have been
631 identified and investigated with respect to the critical parameters at play. This analysis characterises
632 the irreversibility of the process occurring in real absorbers and has been used to identify the least
633 irreversible value of the solution mass flow rate for various operative conditions. These results make
634 evidence of the importance to work at reduced mass flow rates with a thin uniform film, and
635 consequently, tension-active additives are required to realize this condition.

Furthermore, a simplified and general thermodynamic analysis of the whole system performance has been proposed in order to highlight the important role of irreversibilities σ. This analysis makes evidence of a dimensionless ratio "Q/σT" that separates the weight of the irreversibilities. By maximizing this term the system efficiency is enhanced. Since the duty of the absorber is different in refrigeration or heat boosting applications, two different dimensionless parameters have been defined, *DQ* and *DA*, comparing, respectively, thermal flux at the tube wall and absorption at the interface with entropy generation related to the process.

The following main conclusion can be stated:

- The parametric analysis performed makes evidence that a minimum entropy generation can always be identified in terms of the film Reynolds number.
- The absorber of a chiller and that of a heat transformer work in different operative conditions which determine different irreversibility amounts introduced. In general, entropy generation in the heat transformer operative conditions is lower than that of the chiller and, although the overall trend is conserved, the minima occur at higher Reynolds.
- A bigger radius increases the absolute value of every entropy generation group. Thermal irreversibility E_t highlights a relaxingly-increasing trend with respect to Reynolds number. Contrarily, the vapor diffusion related irreversibility E_d is characterised by a relentlessly decreasing trend. The group related to the coupled effects of mass convection and heat transfer E_c has a critical effect on the global trend of the entropy generation rate per unit length E_G and shows a local minimum, which can be explained considering that, increasing Reynolds number, the velocity field is intensified while absorption heat release is reduced. A bigger outer radius moves the minimum to higher *Re* and to lower values of E_c. Finally, the bigger the tube radius the higher the friction related irreversibility E_f.

- Comparing chiller and heat transformer applications, as a rule, the latter highlights a higher impact of the diffusion related irreversibility.
- A higher difference between the solution inlet and tube wall temperatures increases both heat transfer and, increasing the driving force for vapor absorption, mass transfer at the interface. Accordingly, entropy generation is higher when this temperature difference is increased, while the optimal Reynolds is weakly dependent on this parameter.
- When the inlet solution is at thermodynamic equilibrium with the vapor pressure in the absorber, heat transfer at the wall and mass transfer at the film interface (represented through the dimensionless parameters *DQ* and *DA*) can be maximised by a defined value of film Reynolds number. It can be highlighted that the optimal value of this parameter is mainly dependent on the outer tube radius and the application case (i.e chiller or heat transformer operability), while a weak influence of the temperature difference between the inlet and the wall temperature is shown.
- The sub-cooling of the solution moves the occurrence of the maxima to higher Reynolds. Contrarily to the case of thermodynamic equilibrium, when the temperature difference between the inlet and the wall temperatures is changed, *DQ* and *DA* display the occurrence of an optimal condition and higher values of the sub-cooling move the maximum to lower wall temperatures and higher Reynolds. Furthermore, by considering the physical meaning of each parameter and the different operability of the absorber in the two application cases considered, it can be observed that the optimal value of *DA*, at which the absorber operates at the maximum absorption rate with the least thermal power to be rejected, corresponds to the most suitable condition for a chiller or a heat pump, while by maximising *DQ* in the absorber the maximum thermal power is supplied at high temperature and, consistently, a heat transformer operates at its best thermodynamic condition.

683 In conclusion, *DQ* and *DA* practically allow the user to realise a second law optimization of the
684 absorber performance with respect to Reynolds, tube radius and cooling water temperature, by
685 taking into account entropy generation. Also their influence on the overall system performance has
686 been suggested.

687 ## References

688 *[1] A. Bejan, The thermodynamic design of heat and mass transfer processes and devices,*
689 *International Journal of Heat and Fluid Flow, 8, 4, (1987), 258-276.*

690 *[2] P. A. N. Wouagfack, R. Tchinda, Finite-time thermodynamics optimization of absorption*
691 *refrigeration systems: A review, Renewable and Sustainable Energy Reviews, 21, (2013), 524-536.*

692 *[3] Feidt M., 2010, Thermodynamics applied to reverse cycle machines, a review, International*
693 *Journal of Refrigeration, 33, 1327-1342*

694 *[4] M. Kilic, O. Kaynakli, Second law-based thermodynamic analysis of water-lithium bromide*
695 *absorption refrigeration system, Energy, 32 (8), (2007), 1505-1512.*

696 *[5] S.C. Kaushik, A. Arora, Energy and exergy analysis of single effect and series flow double*
697 *effect water–lithium bromide absorption refrigeration systems, International Journal of Refrigeration,*
698 *32 (6), (2009), 1247-1258.*

699 *[6] P. Donnellan, E. Byrne, K. Cronin, Internal energy and exergy recovery in high temperature*
700 *application absorption heat transformers, Applied Thermal Engineering, 56 (1–2), (2013), 1-10.*

701 *[7] O. Kaynakli, The first and second law analysis of a lithium bromide/water coil absorber,*
702 *Energy, 33 (5), (2008), 804-816.*

703 *[8] A. Yiğit, A numerical study of heat and mass transfer in falling film absorber, International*
704 *Communications in Heat and Mass Transfer, 26 (2), (1999), 269-278.*

705 *[9] J. W. Andberg , G. C. Vliet, A simplified model for absorption of vapors into liquid films*
706 *flowing over cooled horizontal tubes, ASHRAE Trans, 93, (1987), 2454–66.*
707 *[10] V.D. Papaefthimiou, I.P. Koronaki, D.C. Karampinos, E.D. Rogdakis, A novel approach for*
708 *modelling LiBr–H_2O falling film absorption on cooled horizontal bundle of tubes, International Journal*
709 *of Refrigeration, 35 (4), (2012), 1115-1122.*
710 *[11] K. Banasiak, J. Kozioł, Mathematical modelling of a LiBr–H2O absorption chiller including*
711 *two-dimensional distributions of temperature and concentration fields for heat and mass exchangers,*
712 *International Journal of Thermal Sciences, 48 (9), (2009), 1755-1764.*
713 *[12] F. Babadi, B. Farhanieh, Characteristics of heat and mass transfer in vapor absorption of*
714 *falling film flow on a horizontal tube, International Communications in Heat and Mass Transfer, 32*
715 *(9), (2005), 1253-1265.*
716 *[13] J.Y. San, W.M. Worek, Z. Lavan, Entropy generation in combined heat and mass transfer,*
717 *International Journal of Heat and Mass Transfer, 30, 7, (1987), 1359-1369.*
718 *[14] C.G. Carrington, Z.F. Sun, Second law analysis of combined heat and mass transfer in*
719 *internal and external flows, International Journal of Heat and Fluid Flow, 13, 1, (1992), 65-70.*
720 *[15] G. Prakash Narayan, J. H. Lienhard V, S. M. Zubair, Entropy generation minimization of*
721 *combined heat and mass transfer devices, International Journal of Thermal Sciences, 49, 10,*
722 *(2010), 2057-2066.*
723 *[16] I. Chermiti, N. Hidouri, A.B. Brahim, Entropy generation in gas absorption into a falling*
724 *liquid film, Mechanics Research Communications, 38, 8, (2011), 586-593.*
725 *[17] N. Hidouri, I. Chermiti, A.B. Brahim, Second Law Analysis of a Gas-Liquid Absorption Film,*
726 *Journal of Thermodynamics,(2013), ID 909162,10pp.*

727 *[18] S. K. Choudhury, D. Hisajima, T. Ohuchi, A. Nishiguchi, T.Fukushima, S. Sakaguchi,*
728 *Absorption of vapors into liquid films flowing over cooled horizontal tubes, ASHRAE Trans, 99,*
729 *(1993),81–9.*
730 *[19] L. Harikrishnan, Shaligram Tiwari, M.P. Maiya, Numerical study of heat and mass transfer*
731 *characteristics on a falling film horizontal tubular absorber for R-134a-DMAC, International Journal*
732 *of Thermal Sciences, 50 (2), (2011), 149-159.*
733 *[20] W.G. Vincenti and C.H. Kruger, Jr., Introduction to Physical Gas Dynamics, Wiley, New Yor,*
734 *(1965).*
735 *[21] PROPERTIES OF LITHIUM BROMIDE-WATER SOLUTIONS AT HIGH TEMPERATURES AND*
736 *CONDENSATIONS - PART I. Thermal Conductivity", ASHRAE Trans, 96, (1990).*
737 *[22] G. Grazzini, F. Gori, Entropy parameters for heat exchanger design, International Journal*
738 *of Heat and Mass Transfer, 31, 12, (1988), 2547-2554.*
739 *[23] A. Bejan, The Concept of Irreversibility in Heat Exchanger Design: Counterflow Heat*
740 *Exchangers for Gas-to-Gas Applications, J. Heat Transfer, 99, (1977), 374-380.*
741 *[24] D.P. Sekulić, C.V. Herman, One approach to irreversibility minimization in compact*
742 *crossflow heat exchanger design, International Communications in Heat and Mass Transfer, 13, 1,*
743 *(1986), 23-32.*
744 *[25] H. Pahlavanzadeh, P. Nooriasl, Entropy Generation in Liquid Desiccant Dehumidification*
745 *System, Energy Procedia, 14, (2012), 1855-1860.*
746 *[26] D. La, Y. Li, Y. Dai, T. Ge, R. Wang, Effect of irreversible processes on the thermodynamic*
747 *performance of open-cycle desiccant cooling cycles, Energy Conversion and Management, 67, (2013),*
748 *44-56.*

749 *[27] A. Myat, K. Thu, N. Kim Choon, The experimental investigation on the performance of a*
750 *low temperature waste heat-driven multi-bed desiccant dehumidifier (MBDD) and minimization*
751 *of entropy generation, Applied Thermal Engineering, 39, (2012), 70-77.*
752 *[28] N. Giannetti, A. Rocchetti, K. Saito, S. Yamaguchi, Entropy parameters for desiccant wheel*
753 *design, Applied Thermal Engineering (2014) in Press, Corrected Proof. DOI:*
754 *10.1016/j.applthermaleng.2014.10.025.*
755 *[29] D. S. Ayou, J. C. Bruno, R. Saravanan, A. Coronas, An overview of combined*
756 *absorption power and cooling cycles, Renewable and Sustainable Energy Reviews, 21, (2013), 728-*
757 *748.*
758 *[30] H.Z. Hassan, A.A. Mohamad, A review on solar cold*
759 *production through absorption technology, Renewable and Sustainable Energy Reviews, 16*
760 *(7), (2012), 5331-5348.*
761 *[31] K. Parham, M. Khamooshi, D. B. Kenfack Tematio, M. Yari, U. Atikol, Absorption heat*
762 *transformers – A comprehensive review, Renewable and Sustainable*
763 *Energy Reviews, 34, (2014), 430-452.*
764 *[32] X.Q. Zhai, R.Z. Wang, A review for absorbtion and adsorbtion solar cooling systems in*
765 *China, Renewable and Sustainable Energy Reviews, 13(6-7), (2009), 1523-1531.*
766 *[33] S.C. Kaushik, Akhilesh Arora, Energy and exergy analysis of single effect and series flow*
767 *double effect water–lithium bromide absorption refrigeration systems, International Journal of*
768 *Refrigeration, 32 (6), (2009), 1247-1258.*
769 *[34] R. Gomri, Second law comparison of single effect and double effect vapour absorption*
770 *refrigeration systems, Energy Conversion and Management, 50 (5), (2009), 1279-1287.*
771 *[35] S. Gong, K. G. Boulama, Parametric study of an absorption refrigeration machine using*
772 *advanced exergy analysis, Energy, 76, (2014), 453-467.*

773 *[36] D. Zebbar, S. Kherris, S. Zebbar, K. Mostefa, Thermodynamic optimization of*
774 *an absorption heat transformer, International Journal of Refrigeration, 35 (5), (2012), 1393-1401.*
775 *[37] G. Gutiérrez-Urueta, A. Huicochea, P. Rodríguez-Aumente, W. Rivera,*
776 *Energy and Exergy Analysis of Water-LiBr Absorption Systems with Adiabatic Absorbers for Heating*
777 *and Cooling, Energy Procedia, 57, (2014), 2676-2685.*
778 *[38] P. Donnellan, E. Byrne, J. Oliveira, K. Cronin,*
779 *First and second law multidimensional analysis of a triple absorption heat transformer (TAHT),*
780 *Applied Energy, 113, (2014), 141-151.*